Stress Distribution by Improved Designs of Obturator Frameworks Using Photo-elastic Resin Models. In Vitro Study

LAITH MAHMOUD ABDULHADI AL-SAMAWI
Department of Prosthetic Dentistry
MAHSA University
Jalan SP 2, Bandar Saujana Putra, Selangor
MALAYSIA

AMRO DABOUL
Department of Prosthodontics, Gerodontology and Biomaterials
University Medicine Greifswald
GERMANY

Abstract: - Obturator is a prosthetic appliance that is used to restore irreparable maxillary defects. The frames were supposed to form the infrastructure of the obturator that intends to close the maxillary arch defects. Five main types of maxillary defects according to Aramany classification were selected for this study. 15 different design frameworks were fabricated using Co-Cr dental alloy. The defects were simulated using premade maxillary arch models that were reproduced in photo-elastic resin. The fabricated metal frames were seated on the photo-elastic resin models and then were exposed to standardized stress at 3 different locations on the frames using a global testing machine. A custom made plane polariscope was arranged to provide polarized illumination for the light emission and analysis through the models. The photo-elastic resin models were photographed during loading under the testing machine to display the supporting areas deformation in frontal plane. The results showed that the proposed metallic designs variably distributed the stresses around the abutments and the remaining hard tissues on the photo-elastic models.

Key-Words: - Maxillofacial replacement, obturator design, palatal defect, photo-elastic analysis, maxillary defect.

Received: April 9, 2022. Revised: December 7, 2022. Accepted: January 4, 2023. Published: February 13, 2023.

1 Introduction

The massive structure or tissue loss of maxillary arch due to any reason results in a mutilation of the supporting oral and dental components plus impaired vital oral functions. A prosthetic appliance called obturator is used to replace the missing oral and dental structures in order to restore functions as well as aesthetics for the patient. The support, retention, and stability of the replacing prosthesis depend on the amount, quality and distribution of residual hard and soft tissues. Since functional and parafunctional forces are transmitted to abutment teeth through rests, guiding planes, and retainers, the obturator framework design should be configured in accordance with the movements of the obturator during function. The main objective of the framework design should be primarily oriented toward preservation of the remaining oral structures. Despite the framework design will vary according to the size of the defect, the design objectives remain the same; to distribute or control the functional and parafunctional forces so that each supporting or retaining element can be used to its maximum effectiveness without being stressed beyond its physiological limits and to offer the best biologically and mechanically compatible design.

Photo-elastic stress analysis test allows an experimental design limiting both patient and operator variables. Although photo-elastic analysis has some limitations with respect to its capacity to reproduce the non homogeneous and an-isotropic features of teeth, bone, and periodontal ligament, the technique has been extensively and successfully used in dentistry to study the interaction of tissues (teeth and bone) response under simulating oral load that is induced by prosthetic restorations.

2 Causes of Defects

Acquired maxillary defects can be caused by surgical intervention or massive trauma. Surgically created defects result due to removal of part or all of the maxilla due to tumor or pathology involving the maxillary sinus or the palate [1]. Defects from trauma may be the result of an automobile accident, industrial accident or a gunshot wound [1], [2]. Congenital maxillary defects like cleft lip and palate can be treated by different types of obturator prosthesis. However, the treatment of patients with acquired maxillary defects differs from that of patients with congenital defects because of the abrupt alteration in the physiologic processes involving each condition. [3].

3 Objectives of the study

- To analyze the forces transmitted to the supporting structures around abutment teeth in 5 classes of Aramany classification using photo-elastic models with different framework designs commonly used to restore each defect [4].
-To suggest the most suitable design for each defect that produced the least and most even stress on the remaining teeth and supporting structures.

4 Analysis of Stress Transmission

Photo-elastic stress analysis is based on the property of some transparent materials to exhibit colorful patterns when viewed with polarized light. These patterns occur as the result of alteration of the polarized light by the internal stresses into two waves that travel at different velocities [5].
Photo-elastic stress analysis consists of replicating a test object in a photo-elastic epoxy resin and then applying a load to the photo-elastic test object and viewing the resultant stress patterns by using special polarizing filters in a polariscope [6].
A plane polariscope consists of a light source and polarizing filters. Two types of fringes are revealed by using the plane polariscope. The array of colored patterns is called isochromatic fringes. These fringes are related to stress intensity and their number increases in respond to applied loads. The other fringes are the isoclinics. These fringes superimpose on the isochromatic fringes and are related to the stress direction [5].
The photo-elastic stress analysis technique has been extensively and successfully used in dentistry to study the interaction of tissue response and physical characteristics of implants and prosthetic restorations. In addition, it has been used in studying loads transferred to implants [7], [8], [9], removable partial dentures [10], fixed prosthodontics [11], endodontics [12], [13], [14], and bio-materials properties [15].

5 Principles in photo-elasticity

Light is an electromagnetic vibration similar to radio waves. An incandescent source emits radiant energy which propagates in all directions and contains a whole spectrum of vibrations of different frequencies or wavelengths. Those vibrations are perpendicular to the direction of propagation. A light source emits a train of waves containing vibrations in all perpendicular planes. When a polariscope is used, the introduction of a polarizing filter will allow only one component of these vibrations to be transmitted, which is parallel to the privileges axis of the filter. Such an organized beam is called polarized light. The polariscope arrangement in Fig.1 consists of a light source and two plates of material that polarize light (the polarizer and the analyzer), in which the object being tested is placed between these two plates. The two plates are set with their axes of transmission at 90º, therefore no light is transmitted by the analyzer. [16], [17].

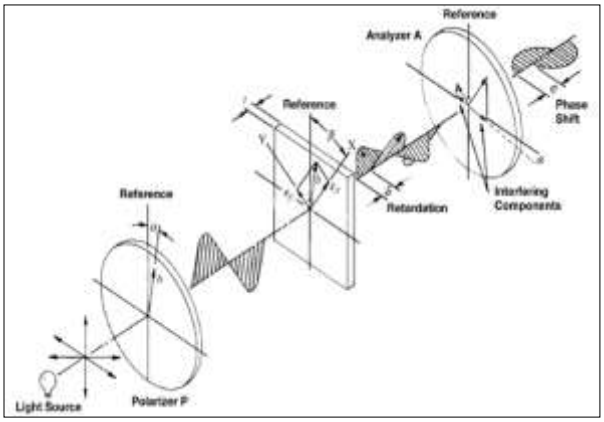

Fig.1 Plane polariscope

Light propagates in a vacuum or in air at a speed (C). In other transparent bodies, the speed (V) is lower and the ratio C⁄V is called the index of refraction. In homogeneous body, this index is constant regardless of the direction of propagation or plane of vibration. Certain materials behave isotropically when unstressed but become optically

anisotropic when stressed. The change in index of refraction is a function of the resulting strain. When a ray of polarized light passes through a photo-elastic material, it gets resolved along the two principal stress directions and each of these components experiences different refractive indices. The difference in the refractive indices leads to a relative phase retardation between the two component waves. The two waves are then brought together in a polariscope. The phenomena of optical interference takes place and a fringe pattern is created, which depends on relative retardation. Thus, studying the fringe pattern can determine the state of stress at various points in the material.

6 Photo-elastic Observations

The photo-elastic technique will provide a visual display of the stresses in a model which are revealed in a polariscope. For most prosthetic appliances, the main information required is the location, distribution and intensity of stress concentrations. Interpretation of the fringes produced in a loaded model follows two main principles: The more the number of fringes produced, the higher the stress intensity, and the closer the fringes are to each other, the higher the stress concentration [5]. A simple interpretation of fringes into stress values is presented in (Fig.2). More than two fringes (> +2) correspond to high stress, from one fringe to two fringes (> +1 to +2) correspond to moderate stress, and less than 1 fringe (< +1) correspond to low stress.

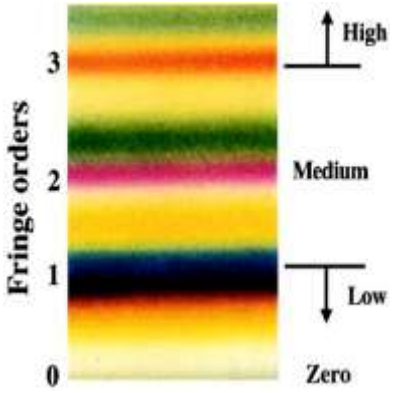

Fig.2 Fringe orders

7 Study Design

Five main types of maxillary defects (Table. 3) were selected. Different framework designs were allocated to each defect type to highlight the most suitable design (Table 1). The designs were tested individually by applying a load of 10 lb. (45 N) to selected loading points on each framework. The models were compared by means of photo-elastic stress analysis to determine the most appropriate design in terms of amount and stress distribution around the abutment teeth.

Classes	Class I	Class II	Class IV	Class V	Class VI
Frames	3	3	4	2	3

Table. 1 Frames and defect types used in the study

7.1 Method

7.1.1 Primary casts preparation

A mold of premade maxillary model (Trimunt. Japan) Fig.3, was prepared using duplication silicone (Wirosil® Bego, Germany). Five custom made blocks were made from auto-polymerizing acrylic resin (Bego. Germany) and were placed inside the initial silicone mold respectively to simulate the defects in each Aramany class. Each acrylic block was designed to simulate an ideal Aramany maxillectomy defect (Fig.3, Fig.4). Working casts with the simulated defects were produced using the modified silicone mold with the acrylic blocks (Fig.3,Fig.4). The resultant casts represented the following defects:

Class I defect: The resection is performed along the midline of the maxilla and teeth are maintained on one side of the arch.

Class II defect: Unilateral maxillary defect that retains the anterior teeth on the contralateral side. The anterior teeth from central to canine are present.

Class IV defect: A defect crosses the midline and involves both sides of the maxilla.

Class V defect: The anterior teeth are preserved and the posterior teeth, hard palate and portions of the soft palate are resected.

Class VI defect: Posterior teeth preserved with the palate, the defect involves the premaxilla.

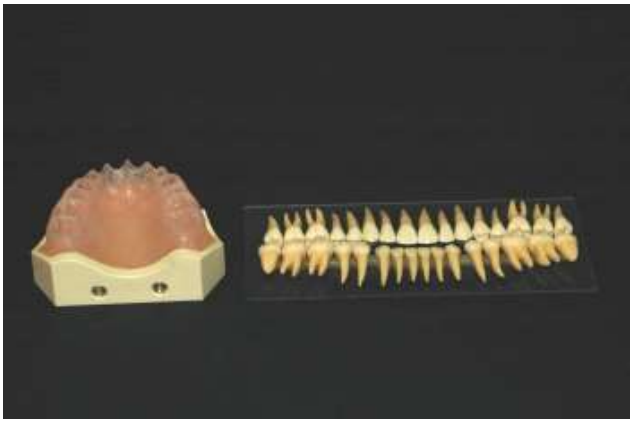
Fig. 3 Premade model used to make defect cast

Later, each primary cast underwent modifications according to the defect type and size using a wax knife and a stone carver to simulate an ideal resection. A mold of each primary cast was made using duplication silicone (Wirosil® Bego. Germany). The models were then relieved approximately 1.5 mm using a graded 3 wheels bur. Light body impression silicone (Wirosil® Bego. Germany) was painted on the relieved casts. The casts were fitted back on the molds before the impression silicone was set to ensure that the impression silicone forms a layer of 1.5 mm thickness simulating the fibromucosa of the palate. A second mold of each primary cast was made with duplicating silicone (Wirosil® duplicating silicone, Bego, Germany) to be used later for producing the photo-elastic models.

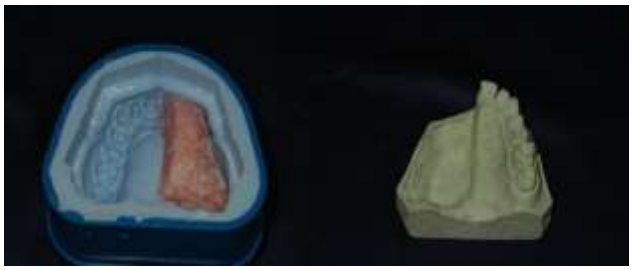
Fig. 4 Example of the fabricated defect stone model

7.1.2 Preparing the testing models

Casting wax sheets (Bego. Germany) of 0.2 mm thickness were used to cover individual teeth roots, stone molds were made for the coated roots. The molds were washed with hot water to eliminate the wax around the teeth and to provide an approximate space of 0.2 mm for silicone mass to be placed to simulate the periodontal ligament Fig.5 [18].
Plastic artificial teeth (B3-305. Trimunt, Japan) were coated with light polyvinyl siloxane impression material (Bego. Germany) in a layer of 0.2 mm to simulate the periodontal ligament, Tray adhesive (Bego. germany) was applied evenly over the roots of the teeth to help fix the siloxane material to the teeth roots. Digital caliper (Mitutoyo Mfg. Japan) Fig.5, was used to check the thickness of the silicone layer. Coated teeth were arranged in the secondary molds, as following:
Class I defect molds: Teeth from central incisor to 2nd molar on the non defect side were preserved.
Class II defect molds: Teeth from the canine on the defect side to 2nd molar on the non defect side were preserved.
Class IV defect molds: 1st and 2nd premolars, 1st and 2nd molars on one side were preserved.
Class V defect molds: Frontal teeth, from 1st premolar to the 1st premolar on the opposing side were preserved.
Class VI defect molds: 2nd premolar, 1st and 2nd molars on both sides were preserved.


Fig.5 fabrication of silicone periodontal ligament


Fig.6 Final photo-elastic model with simulated fibromucosa

7.1.3 Photo-elastic casting

The molds were preheated to 55º C for 30 minutes in a hot air oven (Memmert Gmbh. Germany) to ease the flow of the PL-2 photo-elastic material and reduce the amount of air bubbles. The photo-elastic material was poured into the molds according to the manufacturer's instructions to produce the final photo-elastic testing model

7.1.4 Obturator framework designs

Obturator frameworks were fabricated using Cobalt Chromium (Co – Cr) alloy metal (Bego. Germany) with standardized laboratory methods. The framework designs were made following the general principles:

Occlusal rest seats were prepared with round diamond bur (No.6) with 2.5 mm width, 2.5 mm length and 1.5 mm depth.

The guiding planes on the anterior abutment in occluso gingival height are 2 mm to limit torque on the abutment tooth.

An extension base was fabricated extending into the defect area at the same level of the remaining palate to transmit occlusal forces to the cast in all frameworks.

A bracing component is opposing each retainer.

The following Co-Cr removable partial denture designs were fabricated to replace each defect of the Aramany classification:

Fig. 7- Fig. 21, (B: Bracing arm, R: Retention arm, G: Guiding plane.)

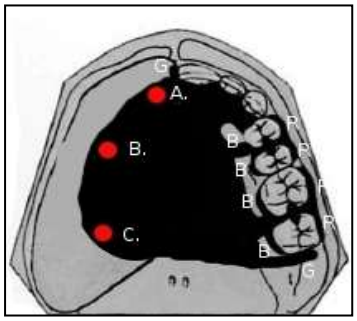

Fig 7 Class I Design 1

A,B,C; stress application points, B; bracing,R; retentive arm,G; guiding plane

-Class I , Design 1; Double embrasure clasp on the molars (distal rest on the 1st molar and mesial rest on the 2nd molar with buccal circumferential cast retainers on the 1st and 2nd molars). Another double embrasure clasp is on the 2nd premolar and 1st premolar. Buccal circumferential cast retainers on the 1st and 2nd premolars Fig.7 [4].

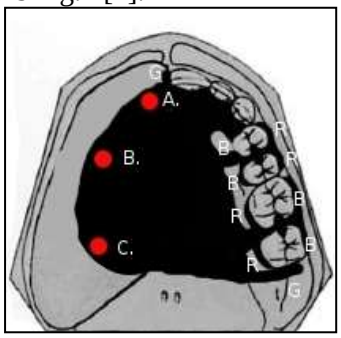

Fig. 8 Class I Design 2

A,B,C; stress application points, B; bracing,R; retentive arm,G; guiding plane

-Class I, Design 2; Embrasure clasp is on the 1st and 2nd premolars with mesial occlusal rest on the 2nd premolar and distal occlusal rest on the 1st premolar. Palatal circumferential cast retainers are on the 1st and 2nd molars with mesial occlusal rest on the 2nd molar and distal occlusal rest on the 1st molar Fig.8 [4].

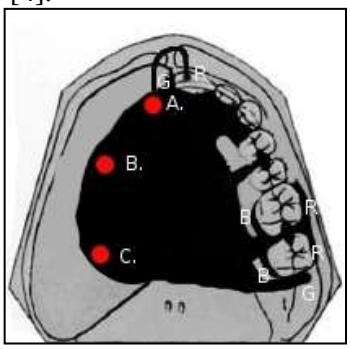

Fig. 9 Class I Design 3

A,B,C; stress application points, B; bracing,R; retentive arm,G; guiding plane

-Class I, Design 3; Buccal circumferential cast retainers are placed on the 1st and 2nd molars with mesial rests on the 2nd molar and distal rests on the 1st molar. Rest seats on the mesial of the 2nd premolar and distal of the 1st premolar with no retentive or bracing arms. I-bar retainer and cingulum rest are on the central incisor Fig.9 [19].

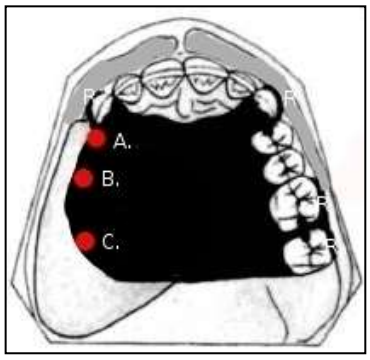

Fig. 10 Class II Design 1

A,B,C; stress application points, B; bracing,R; retentive arm,G; guiding plane

-Class II, Design 1; Buccal circumferential cast retainers are placed on the 1st and 2nd molars with mesial rest on the 2nd molar and distal rest on the 1st molar. A cingulum rest with a buccal cast circumferential retainer is placed on the canine opposing the defect side and on the canine nearest to the defect Fig.10 [19].

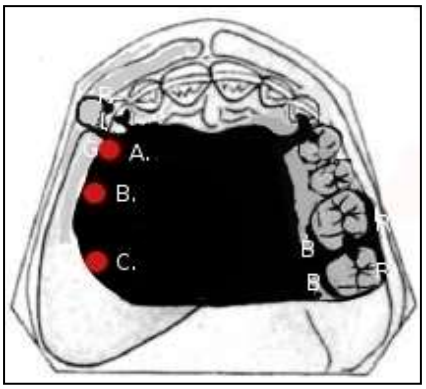

Fig. 11 Class II D
A,B,C; stress application points, B; bracing,R; retentive arm

-Class II, Design 2; Buccal circumferential cast retainers are placed on the 1st and 2nd molars with mesial is located on the 2nd molar and distal rest are placed on the 1st molar. A rest seat is placed on the canine cingulum and a mesial rest on the 1st premolar. I-bar retainer and cingulum rest seat are located on the canine Fig.11.

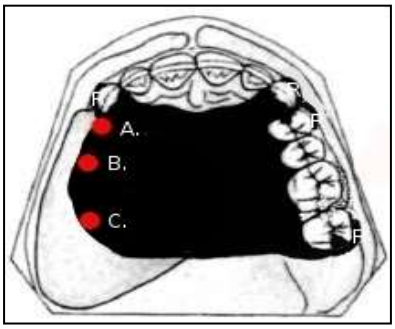

Fig. 12 Class II Design 3
A,B,C; stress application points, B; bracing,R; retentive arm

- Class II, Design 3; A buccal circumferential cast retainer and a distal rest are placed on the 2nd molar, buccal circumferential cast retainers are on the 1st premolar and the canine with rests on the canine cingulum and the mesial of the 1st premolar, a buccal circumferential cast retainer with a rest are placed on the canine nearest the defect Fig.12.

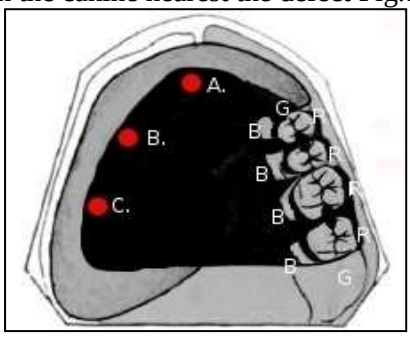

Fig. 13 Class IV Design 1
A,B,C; stress application points, B; bracing,R; retentive arm,G; guiding plane

- Class IV, Design 1; A buccal circumferential cast retainer and a mesial rest are placed on the 2nd molar. A buccal circumferential retainer and distal rest are placed on the 1st molar. Occlusal rest rested on mesial of 2nd premolar and distal 1st premolar with buccal circumferential cast retainers located at 1st and 2nd premolars Fig. 13 [19].

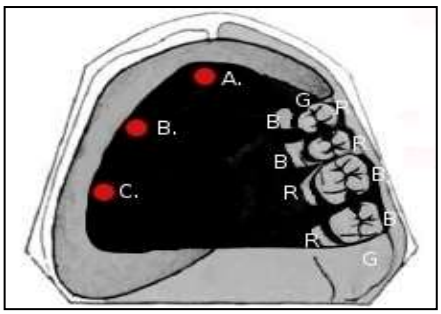

Fig. 14 Class IV Design 2
A,B,C; stress application points, B; bracing,R; retentive arm,G; guiding plane

- Class IV, Design 2; Buccal circumferential cast retainers are put on the 1st and 2nd premolars with mesial rest on the 2nd premolar and distal rest on the 1st premolar. Palatal circumferential cast retainers are placed on the 1st and 2nd molar, mesial rest on the 2nd molar and distal rest on the 1st molar Fig. 14.

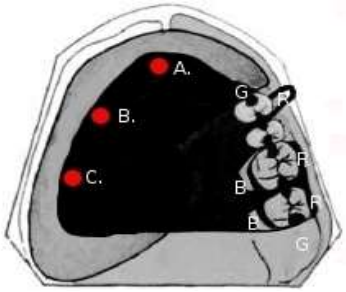

Fig. 15 Class IV Design 3
A,B,C; stress application points, B; bracing,R; retentive arm,G; guiding plane

- Class IV, Design 3; A buccal circumferential retainer, mesial and distal rests placed on 2nd molar, buccal circumferential retainer, mesial and distal rests located on the 1st molar. Mesial and distal rests are on 1st and 2nd premolars with I-bar retainer on the 1st premolar Fig.15.

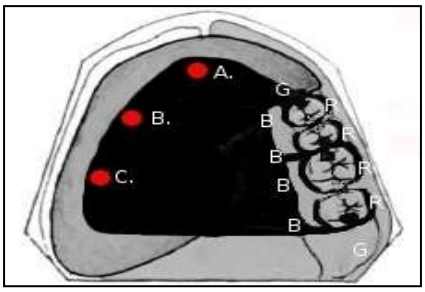

Fig. 16 Class IV Design 4

A,B,C; stress application points, B; bracing,R; retentive arm,G; guiding plane

- Class IV, Design 4; Distal rest with a buccal circumferential cast retainer are placed on the 2nd molar, mesial rest with a buccal circumferential cast retainer are located on 1st molar. Distal rest with buccal circumferential cast retainer are on 2nd premolar, Mesial rest with buccal circumferential cast retainer on 1st premolar (Fig.16). [20].

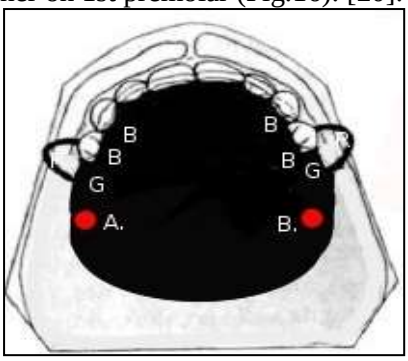

Fig. 17 Class V Design 1

A,B,C; stress application points, B; bracing,R; retentive arm,G; guiding plane

- Class V, Design 1; Cingulum rest placed on both central incisors and both canines, mesial rests with I-bar retainers on both 1st premolars Fig. 17, [4].

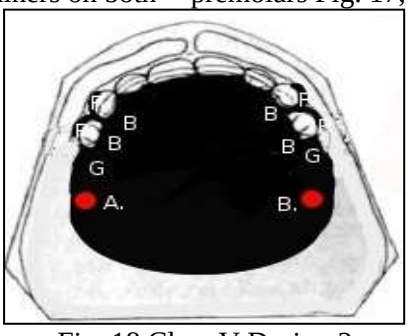

Fig. 18 Class V Design 2

A,B,C; stress application points, B; bracing,R; retentive arm,G; guiding plane

-Class V, Design 2; Cingulum rests are placed on both central incisors, canines and mesial side on the 1st premolars. Buccal circumferential cast retainers are located on the canines and 1st premolars Fig.18.

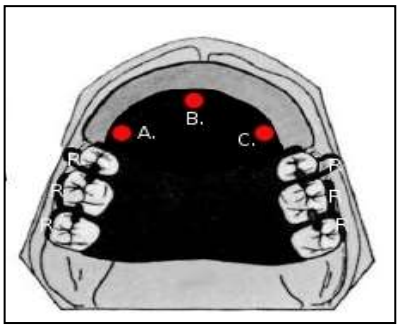

Fig. 19 Class VI Design 1

A,B,C; stress application points, B; bracing,R; retentive arm

-Class VI, Design 1; Buccal circumferential retainers are placed on 1st and 2nd molars with mesial rest is located on 2nd molar and distal rest is on the 1st molar. Mesial rest seats are placed on 1st molar, distal rest with I-bar retainer are located on the 2nd premolar Fig .19

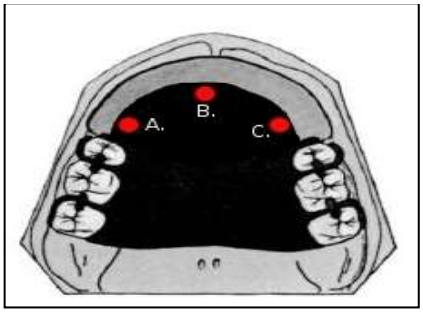

Fig.20 VI Design 2

A,B,C; stress application points, B; bracing,R; retentive arm

- Class VI, Design 2; Mesial rest seats with buccal circumferential cast retainers are located on the 2nd molars with mesial and distal rest seats on the 1st molars, distal rest seats and buccal circumferential cast retainer on the 2nd premolars Fig. 20 [4].

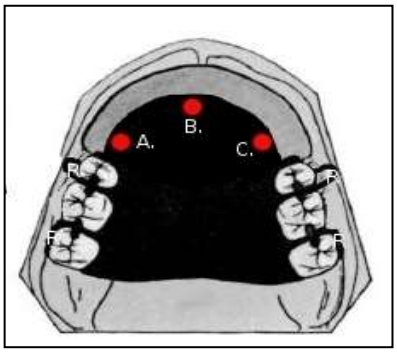

Fig. 21 Class VI Design 3

A,B,C; stress application points, B; bracing,R; retentive arm

- Class VI, Design 3; Distal rest with I-bar cast retainers on the 2nd premolars. Mesial and distal

rest seats on the 1st molars, mesial rest and embrasure on 2nd molar Fig. 21.

7.2 Testing

7.2.1 Application of loads

A load of 10 pounds (45 N) was applied vertically to each loading point respectively by the universal testing machine (Shimadzu co, Japan) Fig. 22. The loads were selected within the realistic functional load levels and also provided a satisfactory optical response in the photo-elastic model [21].
All frameworks shared a similar location of the loading points within the same defect. The loading points for each defect differed according to the size of the defect

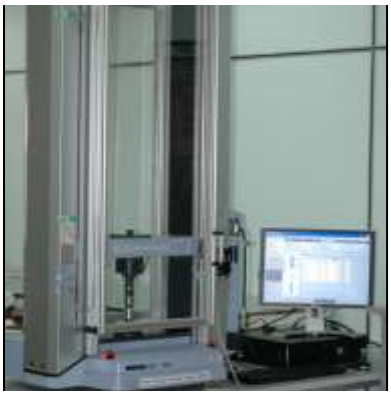

Fig. 22 Universal testing machine

7.2.2 Load application on the obturators

Three points were selected to be the load application on each Obturator used in the study named A, B, C. Fig. 7-Fig. 21. Therefore, the total application number was 3 x15 times.
The photo-elastic model, with its framework, was seated on a custom made base on the lower plate of the universal testing machine (Shimadzu co, Japan. precision was 1/1000 ± 5%). The base was custom made and marked to keep the position of the model during the different load applications Fig.23.

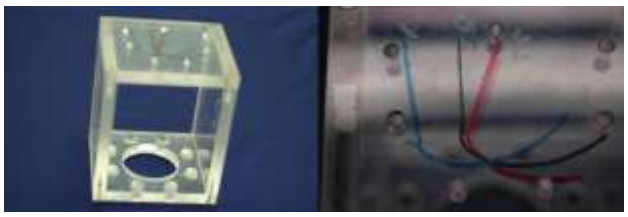

Fig. 23 Custom made base for standardization of model placement

A camera (Olympus E330 EVOLT 8 MP Auto ISO. 14-45 mm / 3.5-5.6 zuiko lens, Japan) was fixed on a tripod stand that offers two fixed reference locations. This permitted taking images of different views of the model while the framework was subjected to loads.
The photo-elastic models showed zero record of stress prior to loading Fig. 24. Each model showed stress fringes when loads were applied and exhibited no stress when the loads were lifted off. Each loading and observation sequence was tested by 2 examiners to ensure reproducibility of the results Table.2. The resultant stresses in all areas of the supporting structure were monitored and recorded photographically in the field of a plane polariscope environment. The polariscope in Fig.25 consists of two polarizing filters and a light source. The light source was a 300 watt tungsten filament with fiber optic extensions.

Fig.24 Testing the model without loading

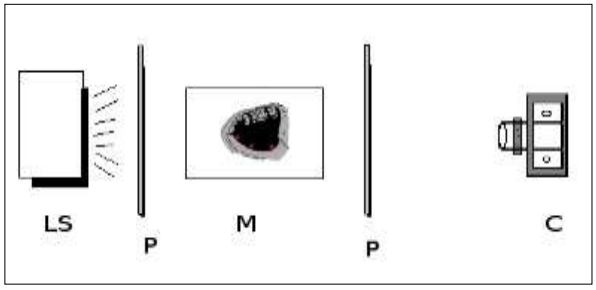

Fig. 25 The arrangement of experiment components (LS; light source; photo-elastic model, P; polarizing filter, C; camera)

7.2.3 Testing and reliability of examiners records

The records of photo-elastic deformation were checked by two examiners instantaneously and a reliability test was carried on to reduce the possible bias between observers using Kappa test,Table. 2.

Observer	Yes	No	Total	Kappa= 0.934 at 95% confidence interval
R1	118	4	122	
R2	118	4	122	

Table.2 inter-examiner reliability

The stress patterns developed by the different designs were compared at the three different loading points using the color chart presented in Fig.2.

7.3 Analysis of fringe records for each frame

The fringes records at different application load points (A, B, C) for each design were added and the total score was compared to other designs. The least stress records by any design were considered the best to be used in treating similar maxillary defect on patients. Since the fringe grading system is qualitative in nature, therefore a qualitative statistical test was used to see the difference among frames of the same Class.

8 Results

8.1 Stress recorded in Class I using 3 different frameworks

Cl I	Cl	LI	C	1Pm	2Pm	1M	2M	Total
D1	0	4	6	4	4	1	0	19
D2	2	5	5	2	4	5	2	25
D3	5	1	5	5	5	2	3	26

Table. 3 Stress records around teeth in Class I, 3 designs (Cl; Class,CI; central incisor, LI; lateral incisor,C;canine,1Pm;1st premolar,2Pm; 2nd premolar,1M;1st molar,2M; 2nd molar).

Results of the statistical analysis for the Class I design using one-Way ANOVA revealed no difference among stresses transmission by the 3 designs (DF=2, F statistic=.571, P-value=.575**).** However, the locations of stresses are variables. We concluded that design 1 may be biologically better than the rest due to that stresses were mainly supported by posterior teeth,Table.3.

8.2 Stress recorded in Class II using 3 different frameworks

Cl II	C	1Pm	1M	2M	Total
D 1	8	6	4	0	18
D 2	6	1	6	1	14
D 3	8	2	1	1	12

Table.4 Stress records in Class II in 2 different designs (Cl; Class, C; canine, 1Pm;1st premolar, 1M;1st molar, 2M; 2nd molar)

The analysis showed absence of mean stress difference among the 3 different designs of frameworks (DF=2, F-statistic =.223, P-value =.804), Table.4. Yet, design 2 and 3 showed reduced stress around teeth in general compared to design 1.

8.3 Stress recorded in Class IV using 4 different frameworks

Cl IV	1 Pm	2 Pm	1 M	2ndM	Total
D1	6	0	2	0	8
D2	8	0	6	1	15
D3	5	0	4	0	9
D4	5	4	4	4	17

Table.5 Stress analysis in Class IV for different designs (1Pm;1st premolar,2Pm; 2nd premolar,1M;1st molar,2M; 2nd molar)

No statistical difference was found among the 4 designs of Class IV (Cl; Class, DF= 3, F statistic= .651, P- value= .597). However, in design 1, the stress concentration areas were reduced around 1st premolar and 1st molar compared to other designs.

8.4 Stress recorded in Class V using 2 different frameworks

Cl V	Cl	C	1Pm	Total
D1	3	0	5	8
D2	1	3	3	7

Table.6 Stress analysis in Class IV for different designs (Cl; Class, CI; central incisor, C; canine, 1Pm; 1st premolar).

In this Class only 2 loading points were used because of the limited area of the remaining arch. Statistical analysis cannot be done for this class due to the limited data. The stress around remaining teeth nearly similar occurrence all teeth nearly affected because of small number, Table.6.

8.5 Stress recorded in Class VI using 4 different frameworks

Cl VI	2Pm	1M	2M	Total
D1	3	4	1	8
D2	3	2	2	7
D3	3	0	0	3

Table. 7 The stress records around teeth using 3 designs in Class VI (Cl; Class,D; design, 2Pm; 2nd premolar, 1M; first molar, 2M; second molar)

The photo-elastic model showed little stress in design 3 due to its configuration that splints the residual teeth altogether, Table 7.

9 Discussions

9.1 photo-elastic of stress analysis

In our practice, this method is commonly used to explore the minimum stress generated by any prosthetic appliance. However, the results are always limited due to the absence of a huge number of oral parameters normally found in the oral cavity like salivary flow, viscoelastic features of mucosa and periodontal ligament, force intensity, direction and neuromuscular reflexes during functional and parafunctional activities. These parameters tend to make the stress resultant unpredictable in reality. Another fact is that the stress amount as represented by a simple scale never reveals the actual intensity of the reaction inside the supporting tissues. Despite all of that this method still offers a good way to reveal the stresses when compared to simulation models.

9.2 Limitations in the fabrication of photo-elastic models

Making an ideal photo-elastic model of the oral cavity with variable components of anatomy and physiology is non-trivial and requires excellent experience to bring it close to actual biological features. However, the results still provide a good vision about what happens around the supporting structures of the obturator during function.

9.3 Analysis

Due to the limited number of the sample in some classes, the statistical analysis gave uncertainty. Therefore, descriptive logic analysis was used to reveal the best design in some classes.

10 Conclusion

The designs that promoted splinting configuration of the remaining supporting teeth showed more even distribution of stresses around the abutments and reduction of concentration to lower number of teeth thus offering more biologically acceptable infrastructure of the obturator. As a conclusion for the best design of obturator infrastructure; in Cl I, D2 and D3 were the best in distributing the stresses around the supporting teeth (posterior teeth). In Cl II, D3 showed reduced stresses around teeth due to the splinting configuration of the abutments. In Cl IV, D1 revealed reduced loads in comparison with other designs. In Cl V, no design preference was obvious and the two models can be used equally. In Cl VI, D3 seems the best due to its splinting capability of the supporting teeth. As a general rule, splinting teeth using any type as a fixed prosthesis or designing the frame to hold the remaining teeth as one unit enhances the stability and retention while directing the functional forces towards the most resistant area of the remaining arch and avoiding high stresses on the alveolar or defect area. The results of this study should proceed with future enhanced frame designs and simulated clinical trials with reconstruction of the defect area to distribute the loads and ameliorate the remaining abutments longevity inside the oral cavity.

References:

[1] Abdulhadi LM, Prosthetic Management and Analysis of Combined Extraoral-Intraoral Maxillofacial Defects Complicated with Microstomia. A Report of Three Cases, *European Journal of Prosthodontics and Restorative Dentistry*, Vol.22, No. 4, 2014, pp 167-173

[2] Wiens JP, Acquired Maxillofacial Defects from Motor Vehicle Accidents: Statistics and Prosthodontic Considerations, *Journal of Prosthetic Dentistry*, Vol. 63, No.2, 1990, pp.172-81.

[3] Desjardins R, Early Rehabilitative Management of the Maxillectomy Patient. *Journal of Prosthetic Dentistry*, Vol.38, No.3, 1977, pp 311-18.

[4] Aramany M, Basic Principles Of Obturator Design for Partially Edentulous Patients. Part II: Design Principles, *Journal of Prosthetic Dentis*try**,** Vol. 40,No.3, 1978, pp 656-62

[5] Caputo A, Standlee JP, *Biomechanics in Clinical Dentistry*, Chicago Quintessence Publ Co., 1987.

[6] Measuremnts Group Tech Note, Tn – 707, 1982.

[7] Ochiai KT, Ozawa A, Caputo A, Nishimura R,() Photo-elastic Stress Analysis Of Implant-Tooth Connected Prostheses With Segmented and Nonsegmented Abutments. *Journal of Prosthetic Dentis*try**,** Vol.89**,** No.5, 2003, pp 495-502

[8] Nishimura R, Ochiai A, Caputo A, Jeong C, () Photo-elastic Stress Analysis Of Load Transfer To Implants And Natural Teeth Comparing Rigid And Semirigid Connectors. *Journal of Prosthetic Dentistry*, Vol.81, No. 6, 1999, pp 696-703.

[9] Gross MD, Nissan J, Samauel R, Stress Distribution Around Maxillary Implants In Anatomic Photo-elastic Models of Varying Geometry. Part I. *Journal of Prosthetic Dentis*try, Vol.85, No.6, pp 442-49.

[10] Thompson WD, Kratochvil J, Caputo A, () Evaluation of Photo-elastic Stress Patterns Produced By Various Designs of Bilateral Distal-Extension Removable Partial Dentures. *Journal of Prosthetic Dentistry*, Vol.91, No. 2, 2004, pp105-13.

[11] Craig RG, Ebrachi MK, Peyton FA, Stress Distribution in Porcelain Fused to Gold Crowns and Preparations Constructed With Photo-elastic Plastics. *Journal of Dental Research*, Vol.50, No. 5, 1971, pp 1278-81.

[12] Cohen BI, Pagnillo M, Musikant BL, Deutsch AS, Comparison of the Retentive And Photo-elastic Properties of Two Prefabricated Endodontic Post Systems. *Journal of Oral Rehabilitatio,* Vol.26, No. 6, 1999, pp 488-94

[13] Asundi A, Kishen A, A Strain Gauge And Photo-elastic Analysis of In Vivo Strain and In Vitro Stress Distribution in Human Dental Supporting Structures. *Archive Oral Biology,*Vol. 45, No. 7: 2000, pp 543-50.

[14] Nakamura A, Teratani T, Itoh H, Sugawara J Ishikawae H, Photo-elastic Stress Analysis of Mandibular Molars Moved Distally with The Skeletal Anchorage System. *American Journal of Orthodontics and Dentofacial Orthopedics*, Vol. 132**,** No.5, 2007,pp 624-29.

[15] Ernst CP, Gerrit R, Klocker K , Willershausen B, by Means of A Photo-elastic Investigation. *Dental Mater*ials,Vol.20, No.4 **,** 2004, pp 313-21.

[16] Abdulhadi LM, *Designing Removable Partial Denture According to Bioprotective Principles*, BPM, 2015.

[17] Orr FJ, Shelton CJ, *Optical Measurement Methods in Biomechanics*, Springer Publications, 1997.

[18] Measurements Group Tech Note, Tn – 702 -2. (2005)

[19] Chou TM, Caputo A, Moore DJ, Xiao B, Photo-elastic Analysis and Comparison of Force-Transmission Characteristics of Intracoronal Attachments with Clasp Distal-Extension Removable Partial Dentures. *Journal of Prosthetic Dentis*try, Vol. 62, No.3, 1989, pp 313-19.

[20] Parr GR, Tharp GE, Rahn AO, Prosthodontic Principles in the Framework Design of Maxillary Obturator Prostheses. *Journal of Prosthetic Dentis*try, Vol. 62, No. 2, 1989, pp 205-12.

[21] Ono T, Kohda H, Hori K, Nokubi T, Masticatory Performance in Postmaxillectomy Patients with Edentulous Maxillae Fitted with Obturator Prostheses, *International Journal of Prosthodonti*cs, Vol. **20**, No.2, 2007, pp145-50

Contribution of Individual Authors to the Creation of a Scientific Article (Ghostwriting Policy)

Abdulhadi LM, carried out the authoring, designing of the experiment, supervision, mathematical analysis, and writing of the article.
Daboul A, has implemented all of technical work and application of the instructions.

Sources of Funding for Research Presented in a Scientific Article or Scientific Article Itself
This work is funded by a grant from University of Malaya.

Conflict of Interest

The authors have no conflicts of interest to declare that are relevant to the content of this article.